Available online at www.sciencedirect.com

ScienceDirect

Procedia CIRP 95 (2020) 138–142

www.elsevier.com/locate/procedia

CIRP Manufacturing Systems Conference 2019

The Jet formation in Ring-shape Laser Induced forward transfer

Yu Deng[a,b,c] *, Yujian Zhang[a] , C.P.Tsui[d] , Zhongning Guo[a] ,Rongli Zhao[a], Sujuan Wang[a]

[a] *State Key Laboratory of Precision Electronic Manufacturing Technology and Equipment, Guangdong University of Technology, Guangzhou, PR China*
[b] *Guangzhou Key Laboratory of Nontraditional Machining and Equipment, Guangzhou, PR China*
[c] *Institute of Medicine and Health, Guangdong Academy of Sciences, Guangzhou, PR China*
[d] *Department of Industrial and Systems Engineering, The Hong Kong Polytechnic University, Huang Hom, Kowloon, Hong Kong, PR China*

* Corresponding author. Tel.: +86-18680507030. *E-mail address:* yu.deng@gdut.edu.cn

Abstract

In this study, ring-shape laser spot was used to induce a ring-shape cavitation aiming to improve the separation accuracy in the laser induced forward transfer (LIFT) process. The roles of laser pulse energy and the size of the ring-shape laser spot on jet formation in LIFT process were theoretically analyzed with ring-shape bubble collapse model established by Lattice Boltzmann Method. The results show that the geometrical symmetry of the ring-shape cavitation blocks the interaction between the inner and outer liquids, leading to higher separation accuracy. The simulation results show that under a specific ratio of internal and external diameter of the ring-shape laser spot, a secondary produced vortex velocity flow can further promote the accuracy of the transferring.

Keywords: ring-shape laser-induced, ring-shape cavitation, liquid transfer, numerical simulation;

1. Introduction

Laser-induced forward transfer (LIFT) is a technique that promotes the separation of object by generating pulsed pressure from laser-induced cavitation. At present, this technology is being applied in the fields of microelectronics [1-2], tissue engineering [3-5] and polymer printing[6-7].In biotechnology, Multiple cells in the suspension are likely to be transferred together with one laser pulse because of their flexible link by the viscosity of the cell culture medium [8].This phenomenon greatly reduces the accuracy of single cell separation. Many researchers have proposed solutions to this problem. Among them, some added reagents to the culture medium to adjust the viscosity of cell suspension to improve the separation accuracy. Gudapati used alginate to increase the viscosity of the cell suspension and achieved single cell separation with a success rate of about 68% [9]. Yu Deng applied glycerol to the cell suspension and obtained 73% success rate of single cell separation [10]. Kingsley completely separate single cells by adding collagen to solidify the cell suspension, by which the interaction between cells is avoided[11].However, Xiong and Kérour é dan showed that alginate combined with intracellular calcium ion resulting in the loss of cell ion, glycerol modified the semipermeable function of the cell membrane leading to the loss of cell activity, while collagen block the oxygen and nutrient solution away from cell, which results in low survival rate of the transferred cells [12-13]. Hence, Brasz used microfluidic chip to wrap single cell and culture medium together as a particle that is transferred in LIFT. The success rate increased to 82%, but the pre wrapping process is time consuming[14]. Researchers also tried to pre-separate cells to achieve cell delivery accuracy. Iino introduced micro square pores to format a physical solid block between cells . By adjusting the diameter,

10.1016/j.procir.2020.01.189

depth and arrangement of micro-pores, only a single cell is seeded in each pore, therefore cells are physically isolated by the pore wall [15]. However, since the array of the pores should be specifically design for cell with varied diameter, the flexibility of this method is reduced.

In this paper, a new method of laser-induced forward transfer using ring-shape laser spot is proposed to improve the accuracy of transferring. The ring-shape laser spot induces a ring-shape cavitation. The pulse pressure waves generated by the cavitation overlap with each other under geometric symmetry to form a convergence effect, which can enhance the central pressure to drive the cell separation, while the lateral force blocks the interaction between the inner and outer solutions of the ring-shape cavitation, which can effectively improve the precision of single cell separation. A lattice Boltzmann model is used to calculate and simulate the ring-shape spot with different pulse energy and the ring-shape. The flow velocity field LIFT is analysed to verify the feasibility of the ring-shape laser spot on improving the accuracy of transferring.

2. Numerical simulation of ring-shape laser induced liquid transfer

2.1. simulation model

According to the results of Mao [16], in LIFT process, a high-pressure cavity is induced by the laser. And based on R. Fabbro [17], the initial pressure of a cavity can be estimated as follows,

$$P(0)=0.01\sqrt{\frac{\alpha Z I_0}{2\alpha+3}} \tag{1}$$

where $P(0)$ is the initial pressure (GPa), α is the energy absorption rate of the sacrificial layer (titanium layer) at laser wavelength of 532 nm , Z is the reduced impact impedance between solid and liquid, I_0 is the energy intensity of the laser (GW/cm^2).And Z can be calculated as follows,

$$\frac{2}{Z}=\frac{1}{Z_1}+\frac{1}{Z_2} \tag{2}$$

here, Z_1 is the impact impedance of solids and Z_2 is liquids the impact impedance of liquid. The impact impedance of materials depends on the density of materials ρ_i and the velocity of shock wave u_i [18]. That is $Z_i=\rho_i u_i$ (g·cm^{-2}s^{-1}).

And I_0 can be calculated according to the following formula,

$$I_0=\frac{4E}{\pi\left(R_2^2-R_1^2\right)\tau} \tag{3}$$

where E is the laser energy (mJ), R_1 is the inner radius of the ring-shape laser spot (μm) and R_2 is the outer radius (μm), τ is the laser pulse width (ns).

At the initial stage of expansion, the shape of cavitation bubble is considered as the shape of the laser spot. Its cross section is combining of two symmetrical located semicircles because of the existence of the solid wall, the substrate. The variation of cavitation bubble is influenced by the pressure inside the bubble, liquid viscosity, surface tension and atmospheric ambient pressure. Rayleigh-Plesset equation [19] is used to describe the cavitation bubble as following,

$$R\ddot{R}+\frac{3}{2}\dot{R}^2+4v\frac{\dot{R}}{R}+2\frac{\sigma}{\rho R}=\frac{P_R(t)-P_\infty(t)}{\rho} \tag{4}$$

here, R is the radius of the semicircle cavity, $\dot{R}$ is the velocity of bubble wall, $\ddot{R}$ is the acceleration of bubble wall, ρ is the density of the liquid (Kg/m^3), σ is the surface tension of the liquid (N/m), v is the viscosity of the liquid (m^2/s), P_∞ is the pressure in the liquid, and P_R is the pressure inside cavitation.

Because the life cycle of the cavitation bubble is short, only tens of millisecond, it can be assumed that there is no heat transfer between the liquid and the cavitation bubble. The process is regarded as adiabatic and the fluid is in a constant temperature environment, so the surface tension and viscosity of the fluid are considered as constant as well [20].

The equation of state of ideal gas is $P_0V_0^\gamma=P_1V_1^\gamma$. Among them, γ is the adiabatic coefficient with a value of 1.3 (superheated water vapor [21]).Therefore, the pressure of the cavity can be calculated by the following formula,

$$P_R(t)=P_R(0)\left(\frac{V(0)}{V(t)}\right)^\gamma=P_R(0)\left(\frac{R(0)}{R(t)}\right)^{3\gamma} \tag{5}$$

where V is the volume of the ring-shape cavity, $R(0)$ is the initial radius of the ring-shape cavity section which depends on the difference between the inner and outer diameter of the laser spot.

In the lattice Boltzmann model of laser-induced liquid transfer, the change of bubble volume is described by the flow entrance, and the parameters of the flow entrance are as follows.

$$F_{\text{in}}(R)=\rho_{\text{air}}\frac{dV}{dt} =\rho_{\text{air}}\frac{d\left\{\pi\int_0^{\frac{R_2-R_1}{2}}\left[\left(\frac{R_2+R_1}{2}+\sqrt{\frac{R_2-R_1}{2}-x^2}\right)^2-\left(\frac{R_2+R_1}{2}-\sqrt{\frac{R_2-R_1}{2}-x^2}\right)^2\right]dx\right\}}{dt} \tag{6}$$

where $F_{in}(R)$ is the rate of inlet flow (Kg/s), ρ_{air} is the air phase density.

The lattice-Boltzmann model is established with the XFlow software, and the dynamical characteristics and velocity field distribution of the jet are simulated. In order to further study the process of liquid transfer and reduce the calculation time of the simulation and considering the geometrical symmetricity the simulating domain is set as 2-D model with width of 0.5mm and height of 4mm as shown in Figure 1. The gas flow rate (Mass Flow) is applied as the entrance condition defined at the location of the ring-shape

spot. The red region (thickness of 50μm) is the liquid and the blue region is the air. The left, right and lower boundary conditions of the model are pressure outlets and they are set as 0 GPa. The black line represents the surface of the titanium layer attached to the liquid target and is set as a solid boundary, namely the wall.

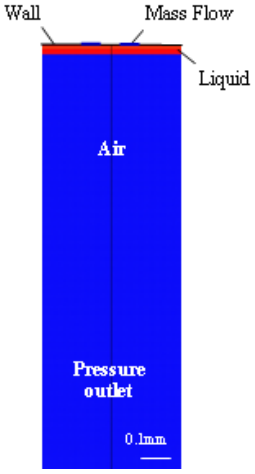

Fig.1. Cross-section of two-phase flow model

2.2. Initial value calculation

The simulation data are shown in Table 1. In the experiment, the sacrificial layer is titanium with the energy absorption rate of 0.48. The sacrificial layer absorbs laser energy in the process but the influence of sacrificial layer on the flow field is not considered in the simulation model.

Table 1. Simulation data

Parameter	data
Laser energy	0.1mJ, 0.2mJ, 0.3mJ, 0.4mJ
Ratio of inner diameter to outer diameter of ring-shape spot	0.75 (112.5μm/150μm), 0.5 (75μm/150μm), 0.25 (37.5μm/150μm)
Laser wavelength	532nm
Laser pulse width	6ns
Energy absorptivity	0.48
Glass Impulse Impedance	2.1×10^{6}g·cm^{-2}s^{-1}
Liquid impulse impedance	0.165×10^{6}g·cm^{-2}s^{-1}
Adiabatic coefficient	1.3
Liquid viscosity	0.423×10^{-3}m^{2}/s
Liquid surface tension	0.0451N/m
Liquid density	1030kg/m^{3}
Liquid thickness	100μm
Air phase density	1.225kg/m^{3}

Fig. 2 illustrates the effect of laser energy and the ratio between the inner diameter and the outer one of the ring-shape spot ($R_r = R_1 / R_2$) on the radius of the cavitation. Because of the extremely high pressure inside the initial bubble, it expands outward dramatically and reaches its maximum volume when the balance between the internal pressure, the pressure of the liquid environment, the surface tension and the inertia of the front-end liquid target is obtained. Since the pressure inside the cavity is lower than the ambient pressure, cavitation bubble begins to contract. When R_r is 0.5, the maximum cavity radius corresponding to laser energy of 0.1mJ, 0.2mJ, 0.3mJ and 0.4mJ are 76μm, 92μm, 100μm and 110μm respectively. Its maximum value all is reached at 30μs. With the increase of the laser energy, the radius of the ring-shape cavity section increases gradually, and the life cycle of the cavity also increases slightly. When the outer diameter of the ring-shape spot remains unchanged at 150 μm, and the decrease of the inner diameter leads to the increase of the laser irradiating area, which enlarges the cavitation. When the laser energy is 0.1mJ, the maximum radius of the cavity corresponding to R_r =0.25, 0.5 and 0.75 are 72μm, 76μm and 82μm respectively.

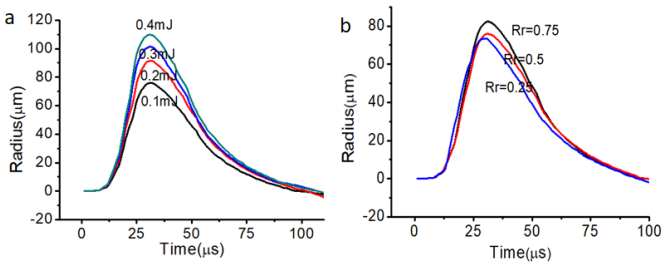

Fig. 2. The variation of the radius of the ring-shape cavity section with time.(a)When R_r = 0.5, the influence of laser energy on the circular radius of ring-shape cavity section ; (b) when laser energy is 0.1 mJ, the effect of R_r value on the circular radius of ring-shape cavitation section.

The entrance conditions are presented in Fig. 3. At the expansion stage, the volume of the cavitation bubble increases continuously, and so the inlet flow rate is positive. At the shrinkage stage, its volume decreases and so the flow rate at the entrance is negative. As can be seen from Figure 3, when R_r is 0.5, the inlet flow velocities of 0.1mJ, 0.2mJ, 0.3mJ and 0.4mJ all reach the maximum value at 43μs, which are 3.6×10^{-6} kg/s, 4.3×10^{-6}kg/s, 4.9×10^{-6} kg/s and 5.4×10^{-6}kg/s respectively. With the increase of laser energy，the inlet flow rate increases gradually. When R_r is 0.75, 0.5 and 0.25, the maximum value of the inlet flow velocity is 2.8×10^{-6} kg/s, 3.6×10^{-6}kg/s and 4.0×10^{-6}kg/s, respectively. The corresponding time of its maximum value is 38μs, 43μs and 52μs respectively. The duration of the maximum velocity increases with the decrease of R_r.

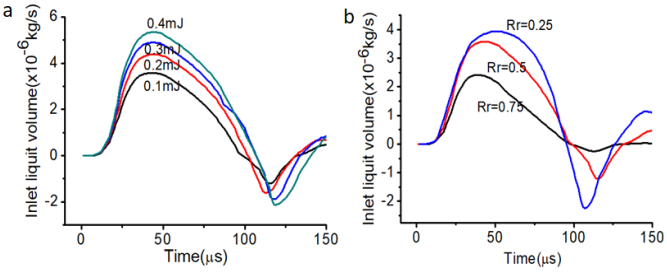

Fig. 3 Inlet flow rate varies with time. (a)the influence of laser energy on inlet flow rate at R_r = 0.5（b）the influence of R_r value on inlet flow rate when laser energy is 0.1 mJ.

3. Simulation result

In order to explore the effect of the ratio of inner to outer diameter of ring-shape spot R_r on the transferring process, the flow field is analysed under the condition that while R_r was set at 0.75, 0.5 and 0.25 while the laser energy was 0.1 mJ. The results are shown in Fig. 4.

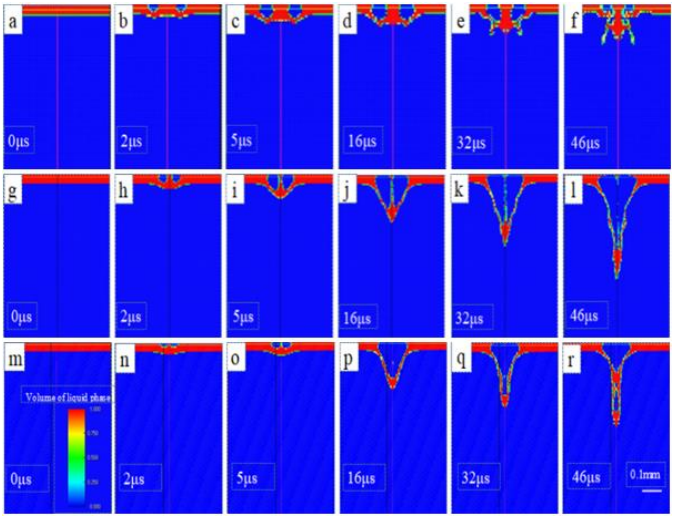

Fig.4 Numerical simulation of liquid transfer with different R_r values. a-f are the numerical simulation of liquid transfer at R_r=0.75. g-l are the numerical simulation of liquid transfer at R_r=0.5. m-r are the numerical simulation of liquid transfer at R_r=0.25.

As shown in Fig. 4 (a-f), when $R_r = 0.75$, at 2μs, cavitation nucleated. With the expansion of the cavity, the target transfer solution in the middle of the ring-shape cavity was isolated at 16μs. At 32μs, only a small amount of target solution is pushed forward, and the energy is not enough to promote the transfer of intermediate target solution. As shown in Fig. 4 (g-l), when R_r=0.5, cavitation nucleated at 2μs. With the expansion of the ring-shape cavity, the intermediate target solution is gradually isolated, and gradually pulled into a slender liquid column to be transferred, shown in Fig.4 h and Fig. 4 j. Then at 16μs, all target solutions were transferred to the front. At 46μs, the ring-shape cavitation bubbles fused together to continue to promote the solution transport. As shown in Fig. 4 (m-r), when $R_r = 0.25$, the target solution has not been completely separated. The ring-shape cavitation bubbles have been fused together in the beginning of ring-shape cavity expansion (5μs-16μs), which has not achieved the result of improving the separation accuracy. To sum up, in the process of cavitation expansion, the liquid under the action of pulse pressure can be divided into two parts of solution with opposite direction of motion, one of which is converged to the inner ring and the other is diffused to the outer ring. It can achieve the complete isolation of the target transfer solution. When the ratio of internal and external radius R_r is relatively small, the pulse pressure converging on the target solution is enough to push the target solution forward, so the separation of the target transfer solution can be achieved.

In order to further explore the contribution of the laser shape, the target is regarded as a particle and its velocity V_p, as shown in Figure 5.

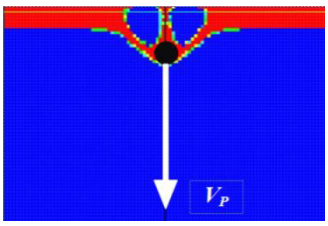

Fig.5 Particle diagram

Fig. 6 shows the velocity change of this particle under different R_r in the bubble expansion stage (1μs -30μs). When R_r = 0.75, the maximum velocity of the target solution is 57m/s at 7.5μs. Then it decreased to 20 m/s and tended to be stable. When R_r = 0.5, the velocity of the target solution reaches 185m/s in the first 4μs and increase to the maximum 195m/s in the following 8μs. Then it began to slow down to 132m/s. When R_r = 0.25, the speed of the target solution reaches the maximum value of 142m/s at the beginning. Then it decreased to 106m/s and tended to be stable. The velocity of R_r = 0.5 curve decreased more slowly than that of R_r = 0.25.

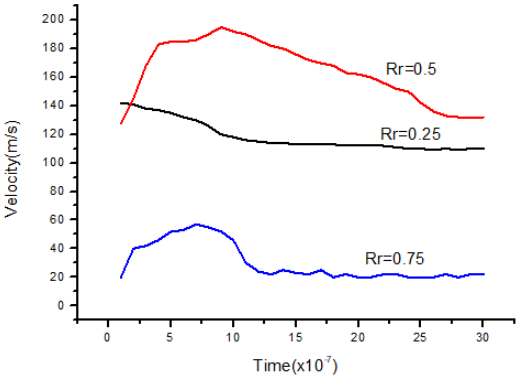

Fig.6 The change of particle velocity with time

4. Flow field velocity analysis

Fig.7（a-e）shows the flow filed at R_r=0.75. At 16μs, the flow velocity is large enough to separate the solution inside and outside the ring. In this case, there is no stable vortex in the bubble expansion stage. At 32μs, some of the target solutions obtained the speed of moving forward, but the further transfer of the target solution was prevented because of the viscosity between the solutions. In Fig.7（f-j）is the flow field at R_r =0.5. A geometrically symmetric vortex appears sooner after the cavitation initiation (Fig.7 g) due to pressure unbalance between the center area and the outer of the cavitation. The target solution in the middle of the ring is pushed out by the symmetric pulse pressure. At 16μs, as the bubble continues to expand, the liquid is blocked by the side solution and a secondary vortex is generated (Fig. 7 h). The new vortex velocity field further promotes the transport of the

target transfer solution. At 32**μs**, the first vortex disappeared, and the second vortex velocity flow has become the main driving force of solution transfer (Fig. 7 i). At 46**μs**, the target transfer solution has been successfully transferred (Fig. 7 j). Fig.7（k-o）illustrates the flow filed at R_r=0.25. In the early stage of cavity expansion, a geometrically symmetric vortex is also formed. However, as the cavity continues to expand until the later stage of expansion, no new vortex appeared. The target transfer solution is driven by the first vortex flow field. From the velocity distribution of the flow field, it is found that the vortex formed in the second time further provides the transmission power for the target transfer solution, while the vortex velocity flow formed in the first time not only promotes the transfer of the target solution, but also part of the driving force acts on the side solution.

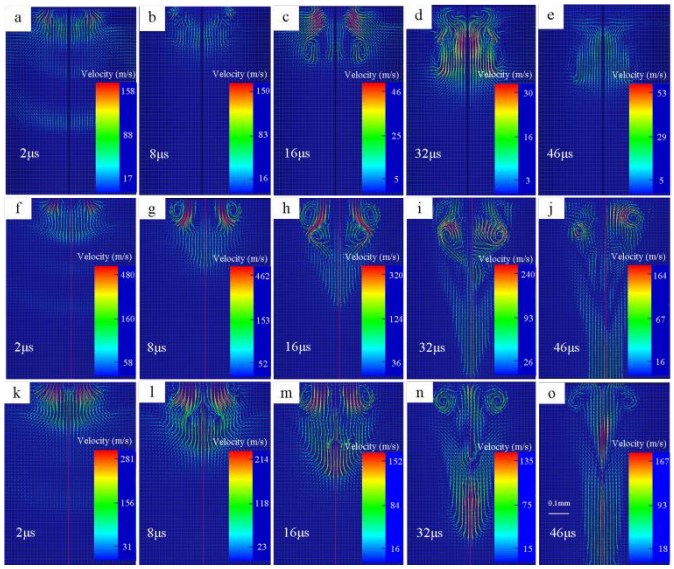

Fig.7 Flow field velocity distribution with different R_r values. a-e are the flow velocity distribution at R_r=0.75. f-j are the flow velocity distribution at R_r=0.5. Figure k-o are the flow velocity distribution at R_r=0.25.

Conclusion

The target solution can be successfully separated in LIFT by using the ring-shape spot. The ring-shape cavitation bubbles cut off the direct interaction between the solution inside and outside the ring and effectively improve the separation accuracy. Under the same pulse laser energy, the smaller ratio of inner diameter to outer diameter of the ring-shape spot induces cavitation bubble, which can push out the solution smoothly under the symmetrical extrusion of pulse pressure. When R_r=0.5, the secondary vortex velocity flow formed in the ring-shape cavitation bubble can further promote the solution transfer.

Acknowledgments

This work was supported by the National natural science foundation of China (51805092), Special fund project of Guangdong academy of sciences to build a first-class research institution in China (2019GDASYL-0103019), the Open Fund of the Key laboratory of High-Incidence-Tumour Prevention & Treatment (Guangxi Medical University) (GKE2019-KF02) and the Research Committee of The Hong Kong Polytechnic University (Project codes: 1-ZVL2 & G-YBVX).

References

[1]Honghui Li, Zhigang Huang, Qingtian Yang, et al. Study on Microstructure of high viscosity silver slurry prepared by laser-induced deposition [J]. Laser and infrared, 2017 (8).
[2]Honghui Li. Research and basic application of laser-induced deposition technology [D]. Guangdong University of technology, 2017.
[3]KaraiskouA,ZergiotiI,FotakisC, et al. Microfabrication of biomaterials bythe sub-ps laser-induced forward transfer process[J]. AppliedSurface Science, 2003, 208(208):245-249.
[4] Koch L, Kuhn S,Sorg H, et al. Laser Printing of Skin Cells and HumanStem Cells[J].Tissue Engineering PartC: Methods,2010, 16(5):847-854.
[5]Ringeisen B R,KimH, Barron J A, et al. Laserprinting of pluripotent embryonal carcinomacells[J]. TissueEngineering, 2004, 10(4):483-491.
[6]Fardel R, Nagel M, Frank Nüesch,et al. Laser forward transfer using a sacrificial layer:Influence of the material properties[J]. Applied SurfaceScience, 2007,254(4):1322-1326.
[7]MitoT, Tsujita T, MasuharaH, et al.Hollowing andTransfer of PolymethylMethacrylate Film Propelled by LaserAblation ofTriazeno PolymerFilm[J].
[8]Deng Y, Renaud P, Guo Z, et al. Single cell isolation process with laser induced forward transfer[J]. Journal of Biological Engineering, 2017, 11(1)
[9]. Gudapati H, Yan J, Huang Y, Chrisey DB, Alginate gelation-induced cell death during laser-assisted cell printing, Biofabrication, 2014, 6(3):035022.
[10]. Yu Deng, Philippe Renaud, Optimizing single cell isolation with laser induced forward transfer with alginate, NanoBioTech Montreux 2014, Montreux,2014.11.17-11.19
[11]. Kingsley D, Dias A, Chrisey D, Corr D. Single-step laser-based fabrication and patterning of cell-encapsulated alginate microbeads, Biofabrication, 2013,5(4):045006.
[12]. Xiong R, Zhang Z, Chai W, Huang Y, Chrisey DB, Freeform drop-on-demand laser printing of 3D alginate and cellular constructs, Biofabrication, 2015,7(4):045011.
[13]. Kérourédan O, Desrus H, Rémy M, Kalisky J, Bourget JM, Amédée-Vilamitjana J, Fricain JC, Catros S, Devillard R, Laser-Assisted Bioprinting for Tissue Engineering, Biomaterials and Nanotechnology for Tissue Engineering, 2016:269.
[14]. Brasz CF, Yang JH, Arnold CB, Tilting of adjacent laser-induced liquid jets,Microfluidics and nanofluidics, 2015, 18(2):185-197.
[15]. Iino T, Hagihara H, Hosokawa Y, Single cell isolation from micro-fluid utilizing femtosecond laser-induced impulsive force, Micro-NanoMechatronics and Human Science (MHS), 2016 International Symposium, IEEE: 2016:1-4.
[16] Mao X, Wen S, Russo R E. Time resolved laser-induced plasma dynamics[J]. Applied Surface Science, 2007, 253(15):6316-6321.
[17] Fabbro R, Fournier J, Ballard P, et al. Physical study of laser-produced plasma in confined geometry[J]. Journal of Applied Physics, 1990, 68(2):775-0.
[18] Sano Y, Mukai N, Okazaki K, et al. Residual stress improvement in metal surface by underwater laser irradiation[J]. Nuclear Instruments & Methods in Physics Research, Section B, (Beam Interactions with Materials and Atoms), 1997, 121(1-4):432-436.
[19] Hilgenfeldt S, Brenner M P, Grossmann S, et al. Analysis of Rayleigh-Plesset dynamics for sonoluminescing bubbles[J]. Journal of Fluid Mechanics, 1998, 365: 171-204.
[20] Chen Yinghuai. Gas-liquid-solid coupling simulation analysis in laser induced manufacturing [D]. Guangdong University of Technology, 2018.
[21] Zhang Xuexue. Foundation of Thermal Engineering. 3rd Edition [M]. Higher Education Press, 2015.